

**NANO EXPRESS**

**Open Access**

# Temperature dependence of sensitized Er<sup>3+</sup> luminescence in silicon-rich oxynitride films

Lingbo Xu, Si Li, Lu Jin, Dongsheng Li and Deren Yang\*

## Abstract

The temperature dependence of sensitized Er<sup>3+</sup> emission via localized states and silicon nanoclusters has been studied to get an insight into the excitation and de-excitation processes in silicon-rich oxynitride films. The thermal quenching of Er<sup>3+</sup> luminescence is elucidated by terms of decay time and effective excitation cross section. The temperature quenching of Er<sup>3+</sup> decay time demonstrates the presence of non-radiative trap states, whose density and energy gap between Er<sup>3+</sup>  $^4I_{13/2}$  excited levels are reduced by high-temperature annealing. The effective excitation cross section initially increases and eventually decreases with temperature, indicating that the energy transfer process is phonon assisted in both samples.

**Keywords:** Erbium; Silicon-rich oxynitride; Luminescence; Temperature dependence; Energy transfer

## Background

Incorporating rare earth (RE) ions into semiconductors and glasses has aroused much research interest in the last decades in view of potential optoelectronic applications [1]. The shielded 4f levels of RE<sup>3+</sup> ions would give rise to optical and electronic phenomena that are almost independent of the host matrix. Among RE ions, Er<sup>3+</sup> is of particular interest due to the  $^4I_{13/2} \rightarrow ^4I_{15/2}$  transition at 1.54 μm, which corresponds to the minimum attenuation in commonly used silica optical fibers. Silicon has been one of the most studied hosts for erbium with the aim of photonic-electronic integration. Erbium in silicon can be efficiently excited through electron–hole pair recombination or by impact of energetic carriers [2,3]. However, luminescence of Er<sup>3+</sup> ions in silicon undergoes a significant thermal quenching due to Auger de-excitation and energy back transfer processes [2,4]. To address such challenge, researchers have tried to embed Er<sup>3+</sup> ions in hosts with larger bandgap [5], such as silicon-rich oxide (SRO) or silicon-rich nitride (SRN) [6-15]. Recently, silicon-rich oxynitride (SRON) materials have been studied as optical platforms for erbium doping [16-19]. Er-doped SRON (Er:SRON) shows intense 1.54-μm photoluminescence (PL), and non-resonant Er excitation

by energy transfer from localized states and silicon nanoclusters (Si-NCs) has been demonstrated [17,19]. In addition, due to the flexibly tunable band structure [20,21], efficient and equivalent carrier injections can be acquired in SRON [22], which acts as a promising host matrix of Er<sup>3+</sup> ions for electrically pumped light-emitting devices. Cueff et al. [14] have systematically compared the electroluminescence (EL) properties of erbium in SiO<sub>2</sub>, Si<sub>3</sub>N<sub>4</sub>, and SiN<sub>x</sub>, and they found that insertion of nitrogen would help enhance electrical conduction at the cost of losses in the external quantum efficiency. The excitation of Er in silicon nitride-based devices is via energy transfer from sensitizers as demonstrated by Yerci et al. [23], and the degraded EL efficiency can be ascribed to the unbalanced carrier injection in silicon nitride. To make a balance between the onset voltage and the EL efficiency, it is helpful to use SRON as the hosts for Er doping. Up to now, the temperature dependence of energy transfer mechanisms in Er:SRON has not been investigated and deserves intensive investigation to engineer efficient light-emitting devices based on Er:SRON.

In this paper, we study the temperature-dependent PL measurements performed on Er:SRON films from 20 to 300 K. Two sets of samples annealed at 600°C and 1,100°C, typically without and with Si-NCs, are chosen. The thermal quenching of Er<sup>3+</sup> PL intensity is elucidated by studying the temperature dependence of Er<sup>3+</sup> decay time and effective excitation cross section.

\* Correspondence: mseyang@zju.edu.cn

State Key Laboratory of Silicon Materials and Department of Materials Science and Engineering, Zhejiang University, Hangzhou 310027, People's Republic of China



## Methods

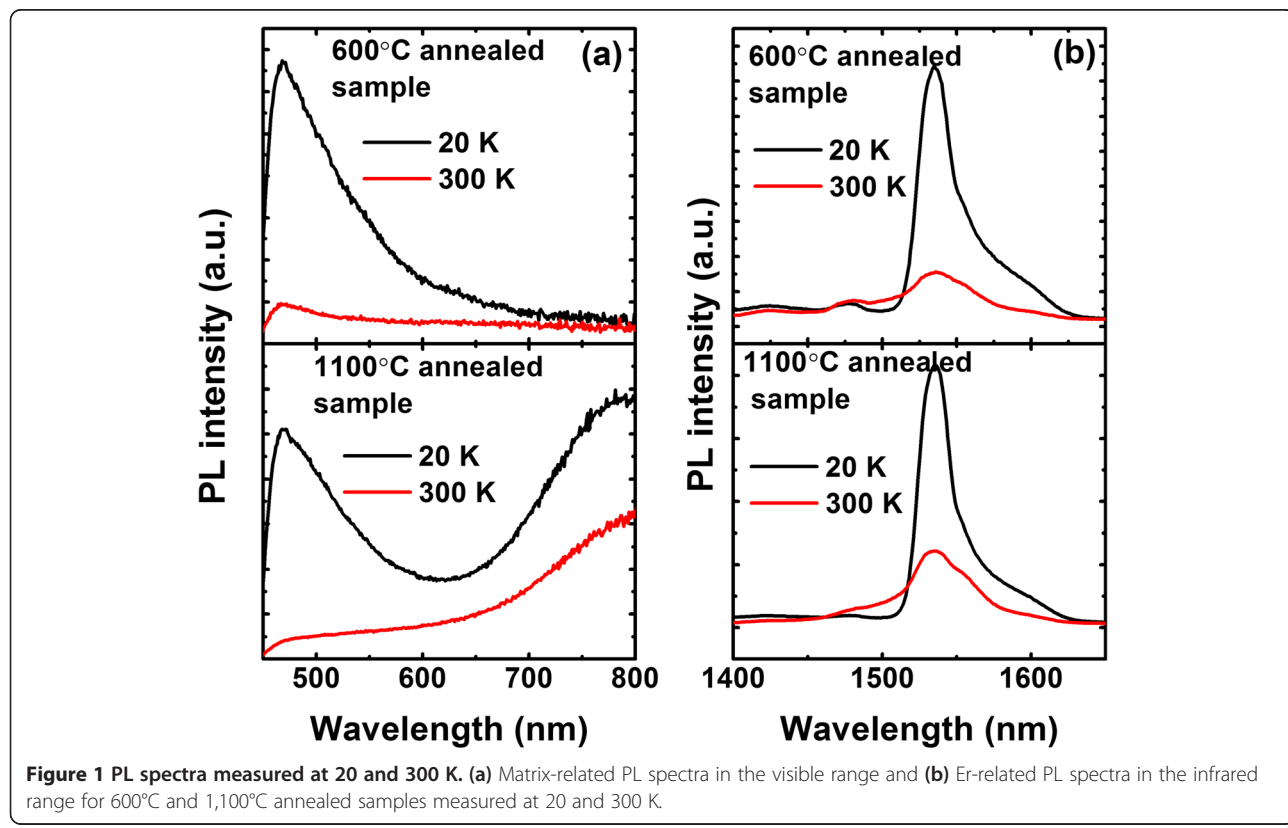
Er:SRON films containing 18 at.% excess Si and 0.4 at.% Er were deposited onto the Si (100) substrates by reactive co-sputtering of Er, Si, and  $\text{Si}_3\text{N}_4$  targets in Ar-diluted 1%  $\text{O}_2$  atmosphere. After deposition, the films were annealed for 1 h under  $\text{N}_2$  flux at 600°C or 1,100°C. Transmission electron microscopy measurements showed the absence of Si aggregates in the 600°C annealed sample, while Si-NCs could be clearly observed in the 1,100°C annealed sample [19]. An Edinburgh Instruments FLS-920 fluorescence spectrophotometer (Edinburgh Instruments, Livingston, UK) was employed, with a xenon lamp as the excitation source in the steady-state PL measurements. A microsecond lamp and a picosecond laser diode were used in the transient PL measurements. The samples were put on the cold finger of a closed-loop He cryostat and kept in a vacuum during the low-temperature measurements. The matrix-related PL spectra were corrected for the system spectra response. A more detailed description of the experimental procedures can be found in [19].

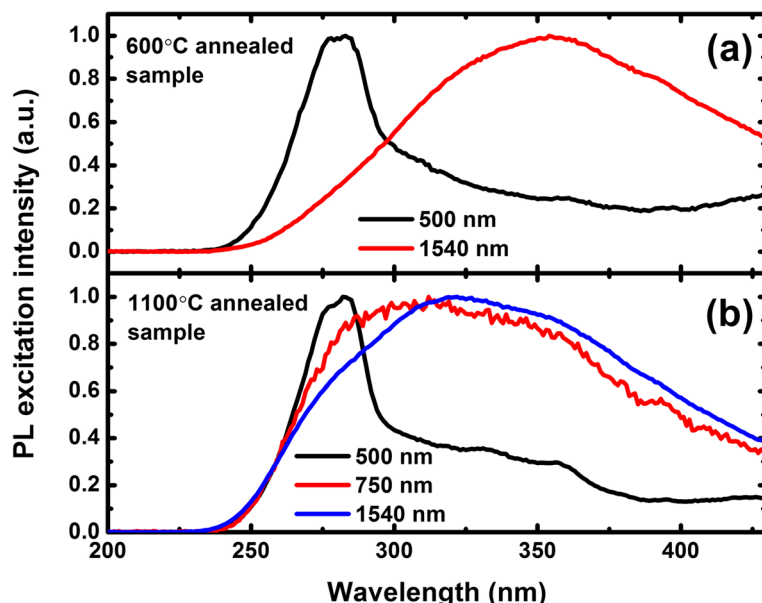
## Results and discussion

Figure 1 shows the PL spectra of the investigated samples measured at 20 and 300 K. Both Er- and Si-NC-related PL bands are observed simultaneously in the 1,100°C annealed sample, while the Si-NC-related PL band is absent in the 600°C annealed sample. At low temperatures, a PL band

centered at approximately 468 nm can be clearly observed in both samples. This band undergoes a significant thermal quenching upon heating, being nearly indistinguishable at 300 K. PL decay measurements show that this band has a characteristic lifetime of about 5 ns, and thus, it is attributed to defect-related luminescence [24,25]. We note that the Er-related emission broadens at room temperature, with more contributions from the higher energy side of the spectra. Indeed, the population redistribution in the crystal-field-split manifold of  ${}^4I_{13/2}$  and  ${}^4I_{15/2}$  sublevels by thermalization gives rise to the observed broadening. Additionally, thermal quenching of Er- and matrix-related PL, commonly ascribed to a competing non-radiative channel on the sensitizers, is observed in both samples. However, the sensitization mechanisms of  $\text{Er}^{3+}$  ions must be clarified before the discussion of thermal dynamics.

Figure 2 shows the normalized PL excitation (PLE) spectra of samples measured at 20 K. PL at wavelengths of 500, 750, and 1,540 nm, typically from defects, Si-NCs, and  $\text{Er}^{3+}$  ions, has been chosen to identify the relationship between their luminescence. The broad PLE bands of  $\text{Er}^{3+}$  ions, with no direct  $\text{Er}^{3+}$  absorption peaks superimposed on, clearly demonstrate the non-resonant excitation of  $\text{Er}^{3+}$  in all the samples. At a glance, we note that the excitation spectra of defect-related PL show an absolutely different wavelength dependence from those of Er-related





**Figure 2** Normalized PL excitation spectra. (a) Normalized PL excitation spectra for PL at 500 and 1,540 nm in the 600°C annealed sample. (b) Normalized PL excitation spectra for PL at 500, 750, and 1,540 nm in the 1,100°C annealed sample.

PL. Contrarily, the PLE spectra of Si-NCs show a similar shape to those of  $\text{Er}^{3+}$  ions. The abovementioned PLE characterization result indicates that the defect-related levels emitting at  $\lambda = 500$  nm are not involved in energy transfer processes, while Si-NCs act as sensitizers for  $\text{Er}^{3+}$  ions in the 1,100°C annealed sample. Moreover, this result suggests that the sensitizers for  $\text{Er}^{3+}$  ions in the 600°C annealed sample are totally dark. We believe that the  $\text{Er}^{3+}$  ions in the 600°C annealed sample are mainly sensitized by the localized states in SRON [19]. The 325-nm excitation peak for PL in the 1,100°C annealed sample is indeed a compromise between the excitation and de-excitation processes of carriers in Si-NCs. The absorption cross section of Si-NCs increases with the energy of incident photons while the radiative recombination probability decreases at the same time, since energetic carriers in Si-NCs suffer from thermalization into efficient non-radiative trap states [13].

Figure 3 shows the temperature dependence of integrated Er-related PL intensity ( $I_{\text{PL}}$ ) for samples annealed at 600°C and 1,100°C in an Arrhenius plot. The PL intensity of the samples is normalized to their values at 20 K.  $I_{\text{PL}}$  drops from 20 K to room temperature by a factor of 3 and 2 for the 600°C and 1,100°C annealed samples, respectively. The thermal quenching of  $\text{Er}^{3+}$  luminescence in SRON is rather small and is comparable to that in SRO [8] as well as in SRN [13]. We try to fit the curves with an Arrhenius equation, yet we find that the fittings do not converge. This indicates that the thermal quenching of sensitized  $\text{Er}^{3+}$  PL in SRON is different from that in SRO and cannot be solely explained by thermal emission of the carriers out

of a confining potential [11]. In the linear excitation regime, we have [26]:

$$I_{\text{PL}} \sim \phi \sigma_{\text{Er}} N_{\text{Er, sen}} \frac{\tau_{\text{dec}}}{\tau_{\text{rad}}} \quad (1)$$

where  $\phi$  is the photon flux,  $\sigma_{\text{Er}}$  is the effective excitation cross section of  $\text{Er}^{3+}$  ions,  $N_{\text{Er, sen}}$  is the density of sensitized  $\text{Er}^{3+}$  ions,  $\tau_{\text{dec}}$  is the decay time, and  $\tau_{\text{rad}}$  is the radiative lifetime. Assuming that  $N_{\text{Er, sen}}$  and  $\tau_{\text{rad}}$  are temperature independent, the reason for the thermal quenching of  $I_{\text{PL}}$  will be elucidated in terms of  $\tau_{\text{dec}}$  and  $\sigma_{\text{Er}}$ .

Figure 4 shows the temperature dependence of  $1/\tau_{\text{dec}}$  for our samples. The samples annealed at 600°C and 1,100°C have  $\tau_{\text{dec}}$  of 0.25 and 0.82 ms at 20 K, respectively. These quantities decrease to 0.11 and 0.47 ms at room temperature, indicating the existence of non-radiative trap states which interact with excited  $\text{Er}^{3+}$  ions. The decay time data can be modeled as follows [13]:

$$1/\tau_{\text{dec}} = W_0 + W_B \exp(-E_A/kT) \quad (2)$$

where  $W_0$  is the decay rate at  $T=0$ ,  $E_A$  is the activation energy of non-radiative trap states, and  $W_B$  is the rate constant of the trap. By fitting the decay data with this model, we obtain that  $W_0$  is 4.2 and 1.2  $\text{ms}^{-1}$ ,  $E_A$  is 12 and 7.8 meV, and  $W_B$  is 7.1 and 1.2  $\text{ms}^{-1}$  in the 600°C and 1,100°C annealed samples, respectively. The value of  $W_0$  for the 600°C annealed sample is larger than that for the 1,100°C annealed sample. This is due to the change in the  $\text{Er}^{3+}$  environment and in the interaction of  $\text{Er}^{3+}$  with the

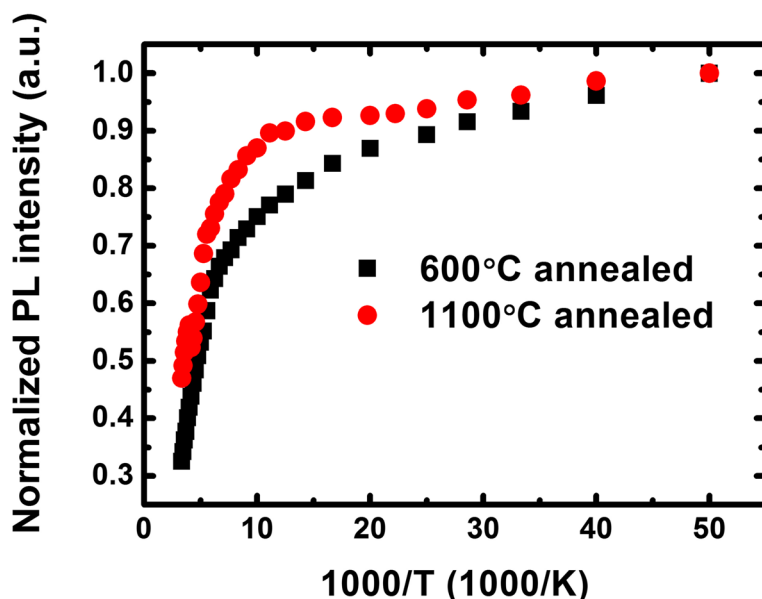


**Figure 3** Emission thermal quenching of Er<sup>3+</sup>. Normalized PL intensity of Er<sup>3+</sup> ions as a function of temperature for the 600°C and 1,100°C annealed samples in an Arrhenius plot.

local field of the embedding medium [27], as it is expected that the 600°C annealed sample is homogeneously amorphous while the 1,100°C annealed sample is phase separated. The decrease of  $E_A$  with increasing annealing temperature indicates the narrowing of energy gap between the Er<sup>3+</sup>  $^4I_{13/2}$  excited level and the trap states, and the decrease of  $W_B$  is ascribed to the gradual passivation of non-radiative trap states during thermal treatments.

After a simple transformation of formula (1), we have formula (3) as follows:

$$\sigma_{\text{Er}} \sim \frac{\tau_{\text{rad}}}{\phi N_{\text{Er,sen}}} \cdot \frac{I_{\text{PL}}}{\tau_{\text{dec}}} \quad (3)$$

Thus, the ratio  $I_{\text{PL}}/\tau_{\text{dec}}$  gives information on  $\sigma_{\text{Er}}$  in relative units, as shown in Figure 5. The  $\sigma_{\text{Er}}$  for the 600°C

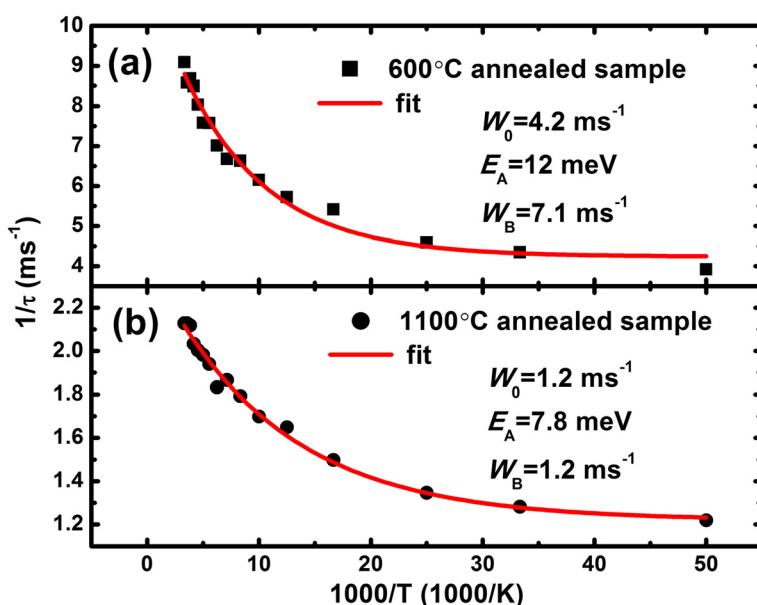


**Figure 4** Temperature dependence of  $1/\tau_{\text{dec}}$ . Temperature dependence of  $1/\tau_{\text{dec}}$  for the 600°C (a) and 1,100°C (b) annealed samples in an Arrhenius plot.

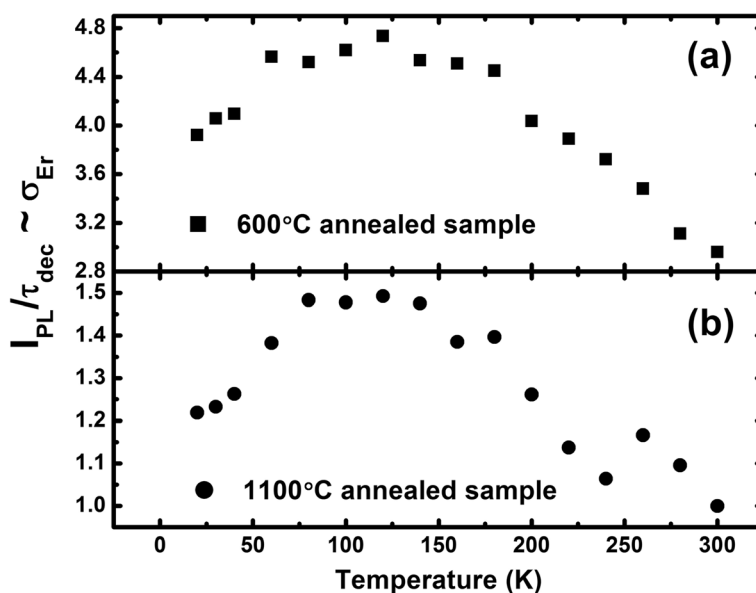


**Figure 5** Temperature dependence of  $\sigma_{Er}$ . Temperature dependence of  $\sigma_{Er}$  for the 600°C (a) and 1,100°C (b) annealed samples.

and 1,100°C annealed samples is found to initially increase with temperature until 140 K before it starts to decrease at higher temperatures. This is similar to the case in Er-doped SRN [13] and implies that the energy transfer process is phonon assisted in both samples, regardless of the sensitization mechanism. For the 1,100°C annealed sample in which the sensitization of  $Er^{3+}$  ions is via Si-NCs, by emitting or absorbing phonons, the momentum conservation rule of electron–hole recombination in Si-NCs is satisfied and the energy mismatch between the recombination energy of excitons and the  $Er^{3+}$  4f-shell energy is bridged [28,29]. For the 600°C annealed sample in which the sensitization of  $Er^{3+}$  ions is via localized states, the localization of an exciton in a small space partially breaks the momentum conservation rule and makes the direct recombination of the exciton possible. However, the energy mismatch may be large, and the increasing number of phonons with temperature is beneficial to bridge it, leading to the increase in energy transfer rate. The temperature dependence of  $\sigma_{Er}$  is thus dominated by the competition between the increasing energy transfer rate and the decreasing excited state density of sensitizers with temperature [13]. Generally, the non-radiative channels are gradually activated with increase in temperature, and their coupling with sensitizers is strengthened, leading to the decrease in excited state density of sensitizers as well as  $\sigma_{Er}$ . It seems that the increase in energy transfer rate is dominant in the low temperature range, while the decrease in the excited state density of sensitizers prevails in the high temperature range.

## Conclusions

In conclusion, we have studied the temperature dependence of sensitized  $Er^{3+}$  emission via localized states and Si-NCs in silicon-rich oxynitride films. Lifetime measurements have proved the existence of non-radiative trap states in both samples, whose density and energy gap between  $Er^{3+} \ ^4I_{13/2}$  excited levels are reduced by high-temperature annealing. Energy transfer from localized states and Si-NCs to  $Er^{3+}$  ions is found to be phonon assisted. The thermal dynamics of  $\sigma_{Er}$  is thus determined by the increasing energy transfer rate and the decreasing excited state density of sensitizers with temperature. Indeed, the thermal quenching of sensitized  $Er^{3+}$  luminescence is small in both samples, indicating that stable room temperature operation of devices based on Er:SRON is possible.

## Abbreviations

Er:SRON: erbium-doped silicon-rich oxynitride;  $I_{PL}$ : Er-related photoluminescence intensity; PL: photoluminescence; PLE: photoluminescence excitation; RE: rare earth; Si-NCs: silicon nanoclusters; SRN: silicon-rich nitride; SRO: silicon-rich oxide; SRON: silicon-rich oxynitride.

## Competing interests

The authors declare that they have no competing interests.

## Authors' contributions

LX carried out the experiments, analyzed the data, and drafted the manuscript; SL and LJ contributed to the analysis of the results in this paper; DL and DY conceived the study, participated in the result discussion, and revised the manuscript. All authors read and approved the final manuscript.

## Acknowledgements

This work was supported by the 973 Program (no. 2013CB632102) and the Innovation Team Project of Zhejiang Province (no. 2009R5005).

Received: 25 July 2014 Accepted: 7 September 2014  
Published: 12 September 2014

## References

1. Kenyon AJ: Recent developments in rare-earth doped materials for optoelectronics. *Prog Quant Electron* 2002, **26**:225–284.
2. Priolo F, Franzò G, Coffa S, Carnera A: Excitation and nonradiative deexcitation processes of Er<sup>3+</sup> in crystalline Si. *Phys Rev B* 1998, **57**:4443–4455.
3. Franzò G, Priolo F, Coffa S, Polman A, Carnera A: Room-temperature electroluminescence from Er-doped crystalline Si. *Appl Phys Lett* 1994, **64**:2235–2237.
4. Prokofiev AA, Yassievich IN, Vrielinck H, Gregorkiewicz T: Theoretical modeling of thermally activated luminescence quenching processes in Si:Er. *Phys Rev B* 2005, **72**:045214.
5. Zanatta AR: Photoluminescence quenching in Er-doped compounds. *Appl Phys Lett* 2003, **82**:1395–1397.
6. Kik PG, Brongersma ML, Polman A: Strong exciton-erbium coupling in Si nanocrystal-doped SiO<sub>2</sub>. *Appl Phys Lett* 2000, **76**:2325–2327.
7. Zhang CS, Xiao HB, Wang YJ, Cheng ZJ, Cheng XL, Zhang F: Photoluminescence thermal quenching behaviors of Er-doped SiO<sub>x</sub> ( $x < 2$ ) prepared by ion implantation. *Phys B* 2005, **362**:208–213.
8. Lin G-R, Lin C-J, Chen C-Y: Enhanced, pumping energy transfer between Si nanocrystals and erbium ions in Si-rich SiO<sub>x</sub> sputtered using Si/Er<sub>2</sub>O<sub>3</sub> encapsulated SiO substrate. *J Nanosci Nanotechnol* 2007, **7**:2847–2851.
9. Saeed S, Timmerman D, Gregorkiewicz T: Dynamics and microscopic origin of fast 1.5 μm emission in Er-doped SiO<sub>2</sub> sensitized with Si nanocrystals. *Phys Rev B* 2011, **83**:155323.
10. Savchyn O, Todi RM, Coffey KR, Kik PG: Observation of temperature-independent internal Er<sup>3+</sup> relaxation efficiency in Si-rich SiO<sub>2</sub> films. *Appl Phys Lett* 2009, **94**:241115.
11. Podhorodecki A, Zatryb G, Golacki L, Misiewicz J, Wojcik J, Mascher P: On the origin of emission and thermal quenching of SRSO:Er<sup>3+</sup> films grown by ECR-PECVD. *Nanoscale Res Lett* 2013, **8**:98.
12. Park N-M, Kim T-Y, Kim SH, Sung GY, Cho KS, Shin JH, Kim B-H, Park S-J, Lee J-K, Nastasi M: Luminescence of Er-doped amorphous silicon quantum dots. *Thin Solid Films* 2005, **475**:231–234.
13. Li R, Yerci S, Dal Negro L: Temperature dependence of the energy transfer from amorphous silicon nitride to Er ions. *Appl Phys Lett* 2009, **95**:041111.
14. Cuetta S, Manel Ramírez J, Kurvits JA, Berencén Y, Zia R, Garrido B, Rizk R, Labbé C: Electroluminescence efficiencies of erbium in silicon-based hosts. *Appl Phys Lett* 2013, **103**:191109.
15. Ramírez JM, Berencén Y, López-Conesa L, Rebled JM, Peiró F, Garrido B: Carrier transport and electroluminescence efficiency of erbium-doped silicon nanocrystal superlattices. *Appl Phys Lett* 2013, **103**:081102.
16. Cuetta S, Labbé C, Khomenkova L, Jambois O, Pellegrino P, Garrido B, Frilay C, Rizk R: Silicon-rich oxynitride hosts for 1.5 μm Er<sup>3+</sup> emission fabricated by reactive and standard RF magnetron sputtering. *Mater Sci Eng B-Adv Funct Solid-State Mater* 2012, **177**:725–728.
17. Xu L, Jin L, Li D, Yang D: Effects of excess silicon on the 1540 nm Er<sup>3+</sup> luminescence in silicon rich oxynitride films. *Appl Phys Lett* 2013, **103**:071101.
18. Steveler E, Rinnert H, Vergnat M: Photoluminescence of erbium in SiO<sub>x</sub>N<sub>y</sub> alloys annealed at high temperature. *J Alloy Compd* 2014, **593**:56–60.
19. Xu L, Jin L, Li D, Yang D: Sensitization of Er<sup>3+</sup> ions in silicon rich oxynitride films: effect of thermal treatments. *Opt Express* 2014, **22**:13022–13028.
20. Huang R, Lin Z, Guo Y, Song C, Wang X, Lin H, Xu L, Song J, Li H: Bright red, orange-yellow and white switching photoluminescence from silicon oxynitride films with fast decay dynamics. *Opt Mater Express* 2014, **4**:205–212.
21. Lin Z, Huang R, Guo Y, Song C, Lin Z, Zhang Y, Wang X, Song J, Li H, Huang X: Near-infrared light emission from Si-rich oxynitride nanostructures. *Opt Mater Express* 2014, **4**:816–822.
22. Wang X, Huang R, Song C, Guo Y, Song J: Effect of barrier layers on electroluminescence from Si/SiO<sub>x</sub>N<sub>y</sub> multilayer structures. *Appl Phys Lett* 2013, **102**:081114.
23. Yerci S, Li R, Dal Negro L: Electroluminescence from Er-doped Si-rich silicon nitride light emitting diodes. *Appl Phys Lett* 2010, **97**:081109.
24. Lin G-R, Lin C-J, Yu K-C: Time-resolved photoluminescence and capacitance-voltage analysis of the neutral vacancy defect in silicon implanted SiO<sub>2</sub> on silicon substrate. *J Appl Phys* 2004, **96**:3025–3027.
25. Lin C-J, Lee C-K, Diau EWG, Lin G-R: Time-resolved photoluminescence analysis of multidoze Si-ion-implanted SiO<sub>2</sub>. *J Electrochem Soc* 2006, **153**:E25–E32.
26. Hijazi K, Rizk R, Cardin J, Khomenkova L, Gourbilleau F: Towards an optimum coupling between Er ions and Si-based sensitizers for integrated active photonics. *J Appl Phys* 2009, **106**:024311.
27. Daldosso N, Navarro-Urrios D, Melchiorri M, Pavesi L, Sada C, Gourbilleau F, Rizk R: Refractive index dependence of the absorption and emission cross sections at 1.54 μm of Er<sup>3+</sup> coupled to Si nanoclusters. *Appl Phys Lett* 2006, **88**:161901.
28. Watanabe K, Fujii M, Hayashi S: Resonant excitation of Er<sup>3+</sup> by the energy transfer from Si nanocrystals. *J Appl Phys* 2001, **90**:4761–4767.
29. Izeddin I, Timmerman D, Gregorkiewicz T, Moskalenko AS, Prokofiev AA, Yassievich IN, Fujii M: Energy transfer in Er-doped SiO<sub>2</sub> sensitized with Si nanocrystals. *Phys Rev B* 2008, **78**:035327.

doi:10.1186/1556-276X-9-489

Cite this article as: Xu et al.: Temperature dependence of sensitized Er<sup>3+</sup> luminescence in silicon-rich oxynitride films. *Nanoscale Research Letters* 2014 **9**:489.

**Submit your manuscript to a SpringerOpen® journal and benefit from:**

- Convenient online submission
- Rigorous peer review
- Immediate publication on acceptance
- Open access: articles freely available online
- High visibility within the field
- Retaining the copyright to your article

Submit your next manuscript at ► [springeropen.com](http://springeropen.com)